

Supplementary Information

Super-thermostable, flexible supercapacitor for ultralight and high performance devices

Dong Won Kim^a, Sung Mi Jung^{b,*}, and Hyun Young Jung^{a,*}

^aDepartment of Energy Engineering, Gyeongnam National University of Science and Technology, Jinju-si, Gyeongnam 52725, South Korea. ^bEnvironmental Fate & Exposure Research Group, Korea Institute of Toxicology, Jinju-si, Gyeongnam 52834, South Korea

* To whom correspondence should be addressed. E-mail: Sungmi.jung@kitox.re.kr, hyjung@gntech.ac.kr

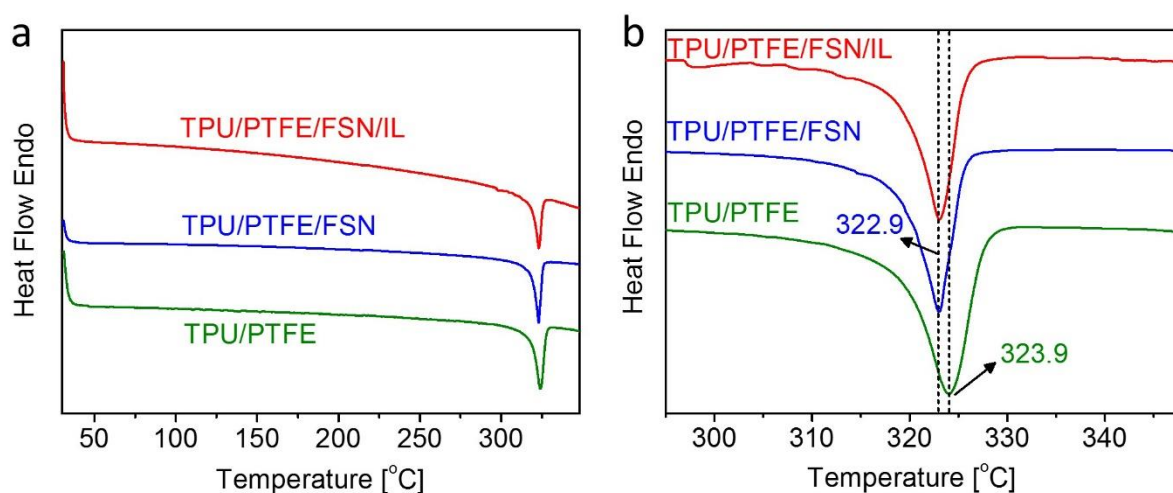


Figure S1. (a) DSC measurements of TPU/PTFE, TPU/PTFE/FSNs, and TPU/PTFE/FSNs/ILs composite electrolytes. (b) The shift in T_m for PTFE.

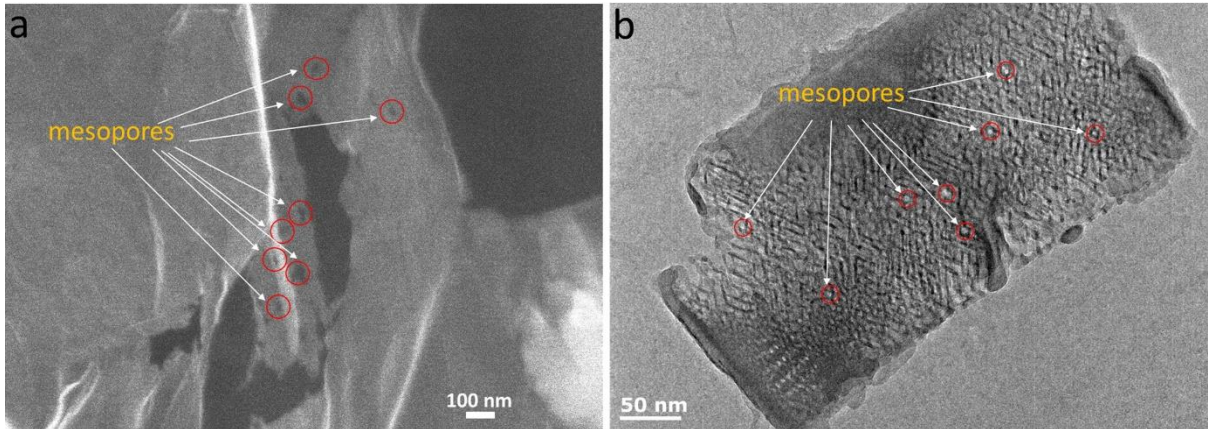


Figure S2. (a) FE-SEM and (b) HR-TEM images showing the mesopores of the graphene aerogels.

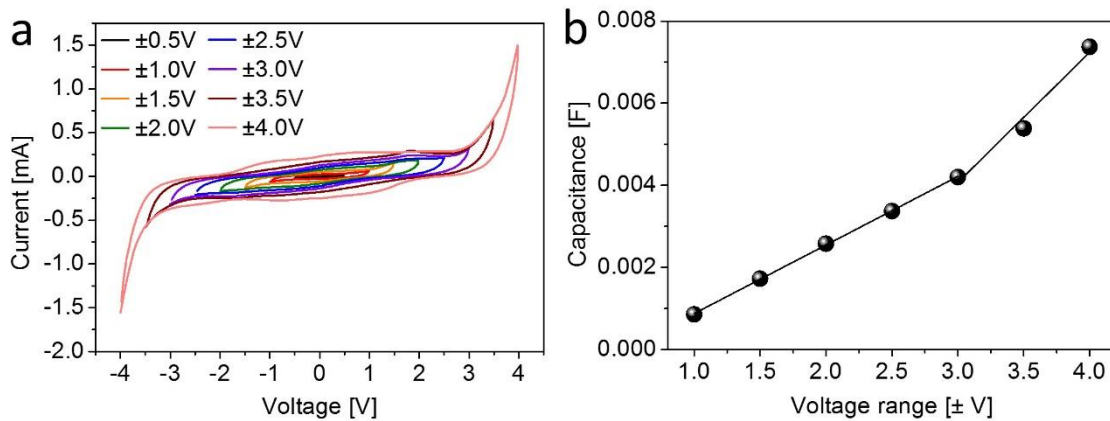


Figure S3. (a) CV measurements as a function of voltage condition in the range of $\pm 4V$, and (b) capacitance values calculated from CV results. To investigate the operating voltage ranges of the composite polymer electrolyte, the measurements have been carried out by using composite polymer electrolytes and the commercial current corrector without active materials.

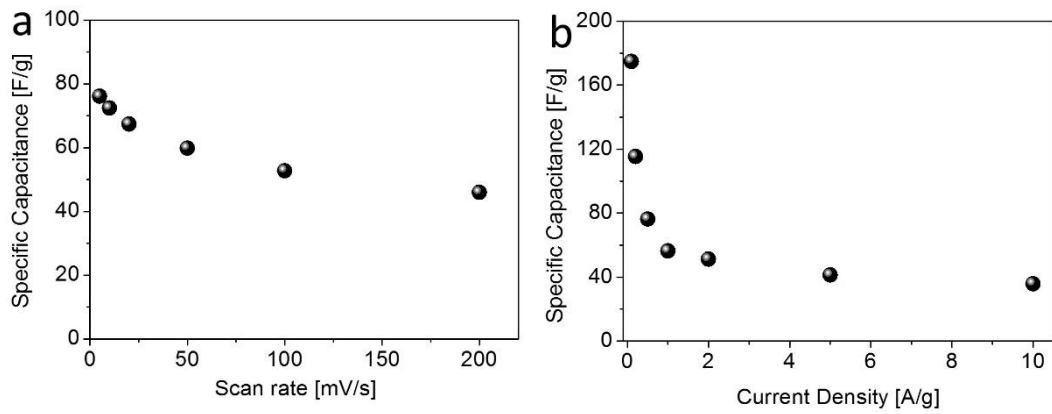


Figure S4. (a) Specific capacitance values calculated from the CV curves of Fig. 3c as a function of various scan rates in the range of 5 to 200 mV/s. (b) Specific capacitance values calculated from the CD curves of Fig. 3d.

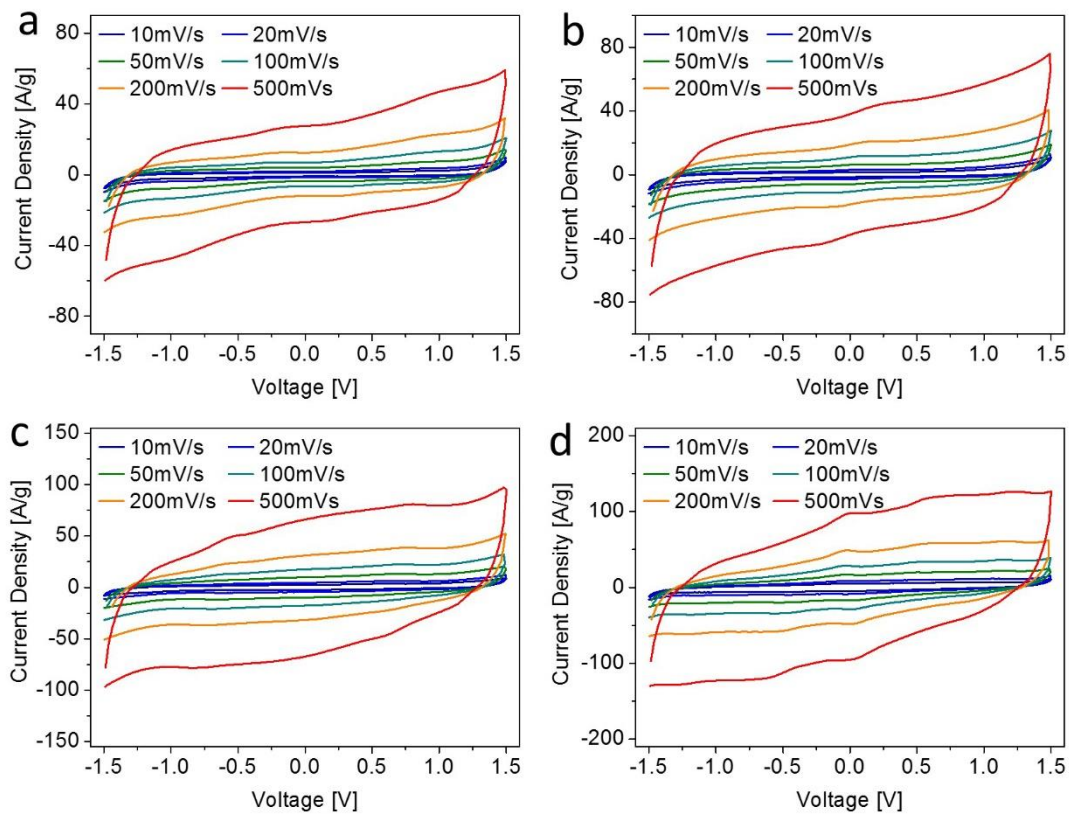


Figure S5. CV profiles as a function of scan rates at 50 °C (a), 80 °C (b), 120 °C (c), and 160 °C (d).

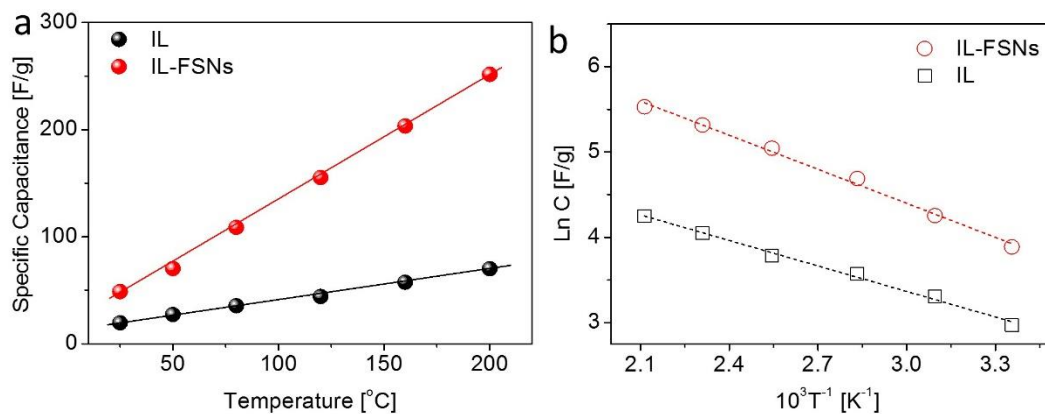


Figure S6. (a) Plots of temperature vs specific capacitance of the supercapacitor device calculated from CV curves of Fig. 4a. (b) Arrhenius plot of specific capacitance calculated from the CV curves vs inverse temperature for the kinetics of ionic transport. The activation energy of the supercapacitor was calculated to be 11 kJ/mol.

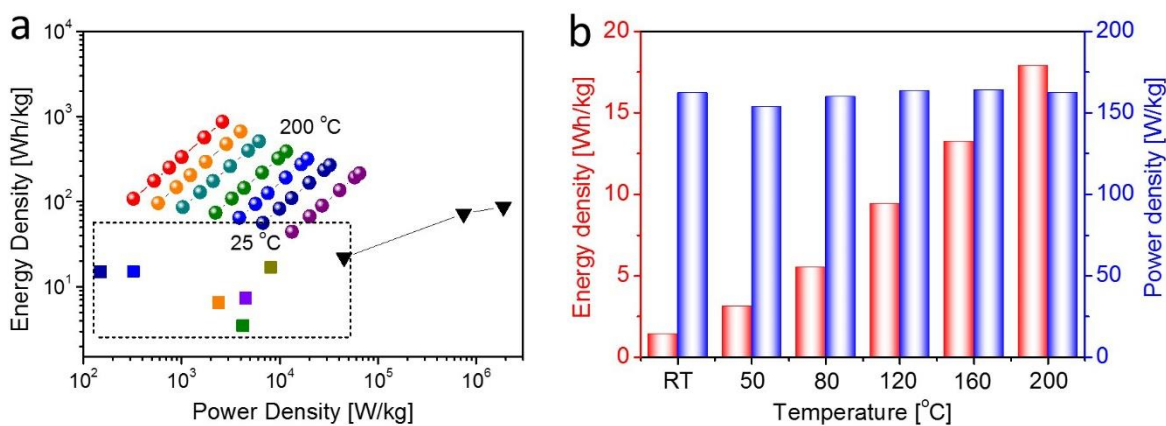


Figure S7. (a) Ragone plots derived from CV measurements of Fig. 4a and 4b, which are compared with previously reported supercapacitors.¹⁻⁵ (b) Energy and power densities calculated using the total mass of devices.

Table S1. Comparison of specific capacitances, and energy and power densities using graphene or CNTs electrodes and IL-based solid-state electrolytes at room temperature.

| Electrode | Electrolyte | OPW[V] | Cs[F/g] | Cycles(retention%) | Es[Wh/kg] | Ps[kW/kg] | Ref |
|-----------------------|--|--------|-----------------|--------------------|-----------|-----------|-------------------|
| Graphene aerogel | IL-FSNs/TPU/PTFE | 0~1.5 | 1007(1A/g) | 10000(>90%) | 1134 | 4.3 | This work(200 °C) |
| Graphene aerogel | IL-FSNs/TPU/PTFE | 0~1.5 | 174 (0.1A/g) | 10000(>95%) | 63 | 3 | This work(25 °C) |
| GNC | EMIMBF4/PVdf-HEP | 0~3.5 | 180(1.0A/g) | 10000(>85%) | 75 | 20 | 6 |
| rGO | BMIMTFSI/TPU/clay | 0~2.5 | 14(2.0A/g) | N/A | 22.118 | 45 | 7 |
| rGO Film | EMIMBF4/c-PVA/c-PHEMA | 0~2.0 | 31(0.1A/g) | 100000(>91%) | N/A | N/A | 8 |
| HEG | BMIMTFSI/PAN | 0~3.0 | 108(1.0A/g) | 1000(>92%) | 30.51 | ~6 | 9 |
| NFC(Gr/CNT buckpaper) | EMIMTFSI/trihoxysilane functional(PEO-PPO-PEO) | 0~3.5 | 78.6(0.2A/g) | 50000(>96.3%) | 66.756 | 0.1756 | 10 |
| Gr doped Carbon | Go doped EMIMBF4/P(Vdf-HFP) | 0~3.5 | 190(1.0A/g) | 5000(>80%) | 76 | 0.84 | 11 |
| rGO | LiClO4/EMIMBF4/BEM/PEO | 0~3.2 | 38.87(0.5A/g) | 5000(>91.2%) | 54.2 | 0.79 | 12 |
| PAGH(Hydrogel) | H2SO4/PVA | 0~1.0 | 248.8(1.0A/g) | 10000(>86.2%) | 26.5 | 0.132 | 13 |
| SWCNT | EMIMBF4/MBAA/DMAA | 0~2.5 | 50.3(0.251A/g) | 5000(>93.4%) | N/A | N/A | 14 |
| MWCNT | EMIMBF4/P(Vdf-HFP) | 0~2.0 | 113.6(0.492A/g) | 8000(>74.0%) | 15.15 | 0.326 | 4 |
| fMWCNT | EMIMFSI/PVDF-HFP/Silica | ± 2.0 | 80.7(0.3A/g) | 2000(91%) | 32.2 | 0.9 | 15 |
| Commercial carbon | EMIMTFSI/P(Vdf-co-HFP) | 0~2.5 | ~140(1.0A/g) | 10000(>97%) | 21.9 | 6.25 | 16 |
| Commercial A.C | BMIM(BF4,TFSI)/VBI(BF4,TFSI)/PEGDA | 0~3.0 | 175.6(1.0A/g) | 10000(>95.2%) | N/A | N/A | 17 |
| Commercial carbon | Go doped EMIMBF4/P(Vdf-HFP) | 0~3.5 | 190(1.0A/g) | 5000(>80%) | 76 | 0.84 | 18 |
| A.C | LiClO4/PAEK/PEG | 0~1.5 | 92.84(0.1A/g) | N/A | 7.4 | 4.5 | 19 |

Table S2. Comparison of specific capacitances and cycle stabilities at various bending angles and/or high temperatures.

| Electrode | Electrolyte | OPW [V] | Temperature [°C] | Bending angle [°] | Capacitance [F/g] | Cycle number | Retention [%] | References |
|-----------------------|--|---------|------------------|-------------------|-------------------|--------------|-----------------|------------|
| rGO Film | EMIMBF4/c-PVA/c-PHEMA | 0~2.0 | 180 | 0 | 88 at 2 A/g | 1,000 | 90.2 at 1.0 A/g | 8 |
| | | | 150 | 60~180 | na | 100,000 | 91 at 2.0 A/g | 8 |
| rGO-PBI | H3PO4 doped PBI | ± 0.5 | 160 | 0 | 170 at 50 mV/s | 100,000 | 93 at 3.6 A/g | 20 |
| | | | 120 | 60~180 | na | 1,000 | 100 at 1.0 A/g | 20 |
| A.C | LiClO4/PAEK/PEG | 0~1.5 | 120 | 0 | 103.17 at 0.1 A/g | 2,000 | 90.8 at 0.5 A/g | 18 |
| A.C | EMIMTFSI in glass-fiber membrane | 0~2.5 | 120 | 0 | 107 at 1.0 A/g | 10,000 | 75 at 5.0 A/g | 21 |
| | | | 120 | Rc=0.05~0.2 mm | na | 400 | 100 at 1.0 A/g | 21 |
| A.C | TMSPMIMCl/pPBI | 0~1.0 | 120 | 0 | 85.5 at 0.05 A/g | 10,000 at RT | 91.0 at 1.0 A/g | 22 |
| A.C | BMIM(BF4,TFSI)/VBI(BF4,TFSI)/PEGDA | 0~3.0 | 120 | 0 | 277.4 at 1.0 A/g | 5,000 at RT | 95.2 at 1.0 A/g | 16 |
| CNG | EMIMBF4/PVdf-HFP | 0~3.5 | 25 | 0~180 | 180 at 1.0 A/g | 1,000 | 88.3 at 1.0A/g | 6 |
| NFC(Gr/CNT buckpaper) | EMIMTFSI/trihoxysilane functional(PEO-PPO-PEO) | 0~3.5 | 25 | Rc=3~10 mm | 78.6 AT 0.2 A/g | 50,000 | 98.4 at 0.2 A/g | 10 |

References

1. R. Borges, A. L. M. Reddy, M.-T. F. Rodrigues, H. Gullapalli, K. Balakrishnan, G. G. Silva, P. M. Ajayan, *Sci. Rep.*, 2013, **3**, 2572.
2. G. P. Pandey, S. A. Hashmi, *J. Mater. Chem. A*, 2013, **1**, 3372.
3. W. Lu, K. Henry, C. Turchi, J. Pellegrino, *J. Electrochem. Soc.*, 2008, **155**, A361.
4. P. Pal, A. Ghosh, *J. Power Sources*, 2018, **406**, 128.
5. T. Y. Kim, H. W. Lee, M. Stoller, D. R. Dreyer, C. W. Bielawski, R. S. Ruoff, K. S. Suh, *ACS Nano*, 2011, **5**, 436.
6. L. Feng, K. Wang, X. Zhang, X. Sun, C. Li, X. Ge and Y. Ma, *Adv. Funct. Mater.*, 2018, **28**, 1704463.
7. R. S. Borges, A. L. M. Reddy, M.-T. F. Rodrigues, H. Gullapalli, K. Balakrishnan, G. G. Silva, P. M. Ajayan, *Sci. Rep.*, 2013, **3**, 2572.
8. H. H. Rana, J. H. Park, E. Ducrot, H. Park, M. Kota, T. H. Han, J. Y. Lee, J. Kim, J. H. Kim, P. Howlett, M. Forsyth, D. MacFarlane, H. S. Park, *Energy Storage Materials.*, 2019, **19**, 197.
9. P. Tamilarasan, S. Ramaprabhu, *Energy.*, 2013, **51**, 374.
10. Y. J. Choi, D. S. Jung, J. H. Han, G.-W. Lee, S. E. Wang, Y. H. Kim, B. H. Park, D. H. Suh, T.-H. Kim, K.-B. Kim, *Energy Technol.*, 2019, **7**, 1900014.
11. X. Yang, L. Zhang, F. Zhang, T. F. Zhang, Y. Huang, Y. S. Chen, *Carbon.*, 2014, **72**, 381.
12. M. Jin, Y. Zhang, C. Yan, Y. Fu, Y. Guo, X. Ma, *ACS Appl. Mater. Interfaces.*, 2018, **10**, 39570.

13. X. B. Liu, S. Zhou, K. X. Liu, C. Lv, Z. P. Wu, T. H. Yin, T. X. Liang, Z. L. Xie, *J. Power Sources.*, 2018, **384**, 214.
14. C. Yin, X. Liu, J. Wei, R. Tan, J. Zhou, M. Ouyang, H. Wang, S. J. Cooper, B. Wu, C. George and Q. Wang, *J. Mater. Chem. A.*, 2019, **7**, 8826.
15. X. Zhang, M. Kar, T. C. Mendes, Y. Wu, D. R. MacFarlane, *Adv. Energy Mater.*, 2018, **8**, 1702702.
16. H. Li, Z. Feng, K. Zhao, Z. Wang, J. Liu, J. Liu, H. Song, *Nanoscale.*, 2019, **11**, 3689.
17. X. Yang, F. Zhang, L. Zhang, T. F. Zhang, Y. Huang, Y. S. Chen, *Adv. Funct. Mater.*, 2013, **23**, 3353.
18. R. Na, P. Huo, X. Zhang, S. Zhang, Y. Du, K. Zhu, Y. Lu, M. Zhang, J. Luan and G. Wang, *RSC Adv.*, 2016, **6**, 65186.
19. D. Kim, P. K. Kannan and C.-H. Chung, *ChemistrySelect.*, 2018, **3**, 2190.
20. S.-K. Kim, H. J. Kim, J.-C. Lee, P. V. Braun and H. S. Park, *ACS Nano*, 2015, **9**, 8569-8577.
21. B. Qin, X. Wang, D. Sui, T. Zhang, M. Zhang, Z. Sun, Z. Ge, Y. Xie, Y. Zhou, Y. Ren, Y. Han and Y. Ma, Y. Chen, *Energy Technol.*, 2017, **5**, 1-11.
22. T. Mao, S. Wang, X. Wang, F. Liu, J. Li, H. Chen, D. Wang, G. Liu, J. Xu and Z. Wang, *ACS Appl. Mater. Interfaces*, 2019, **11**, 17742-17750.